



Transparent and conductive F-Doped SnO₂ nanostructured thin films by sequential nebulizer spray pyrolysis

T. M. W. J. Bandara¹ · A. A. A. P. Aththanayake¹ · G. R. A. Kumara² · P. Samarasekara¹ · L. Ajith DeSilva³ · K. Tennakone^{2,4}

Received: 17 December 2020 / Accepted: 21 January 2021 / Published online: 1 February 2021
© The Author(s), under exclusive licence to The Materials Research Society 2021

Abstract

Transparent conductive oxides (TCOs) are a key component in many optoelectronic applications such as solar cells, flat panel displays, sensors, touch screens, light-emitting diodes, frost-resistant surfaces, and smart windows. The high electronic conductivity and high optical transmission are essential properties of TCOs for these applications. Owing to chemical inertness and high-temperature tolerance, F-doped tin oxide (FTO) films have much demand in a variety of electrochemical devices. In this work, transparent and electrically conductive FTO thin films are prepared on soda-lime glass substrates. The films are fabricated by sequential nebulized spray pyrolysis with the help of a homemade low-cost spray gun. The surface morphology of the films is analyzed using scanning electron micrographs (SEMs). It is found that the surface is homogeneous and FTO crystallite sizes are in the order of ~ 10 nm. XRD pattern of the FTO films exhibits 2θ peaks for corresponding SnO₂ crystal planes at 26.64° (110), 33.90° (101), 37.95° (200), 51.87° (211), 56.17° (200), 60.05° (310), 61.89° (301). The crystallite sizes calculated from XRD data are in agreement with that of SEM. Optical transparency and bandgap energies are evaluated by UV visible spectroscopy. The FTO films with 15 Ω cm⁻² sheet resistance were used to prepare quasi-solid-state dye-sensitized solar cells with a TiO₂ photoelectrode. The solar cell showed a ~ 5% energy conversion efficiency with high short-term stability.

Keywords FTO · Transparent conductive oxides · Nebulized spray pyrolysis · Sheet resistance · Optical transmittance · Solar cell

Introduction

Optically transparent electronically conductive glasses doped with composite metal oxides are important components in many applications [1–3]. Transparent conductive oxide (TCO) films are widely used in photovoltaic solar cells, photoelectrochemical solar cells, flat panel displays, touch screens, light-emitting diodes, smart windows, gas

sensors, and frost-resistant surfaces [4, 5]. Most of these films are doped with polycrystalline or amorphous microstructures of metal oxides. This doping process improves the electrical conductivity of the films, and optical transparency is attained by the wide bandgap (> 3.2 eV) of the material.

Today, commonly utilized transparent conducting oxides are made out of n-type semiconducting materials in which the majority of the charge carriers are electrons supplied by donor atoms. N-doped wide bandgap semiconductors have relatively higher conductivity since the electron have higher mobility than that of holes [6, 7]. For example, Sb- or F-doped SnO₂ and Sn-doped In₂O₃ (indium tin oxide) films are the most common and practically viable TCOs. Some TCOs have also been prepared by composites of binary metal oxides (binary compounds) such as SnO₂ and In₂O₃ without adding impurities or dopants; however, the temperature tolerance of these materials is found to be poor [2, 8]. Indium tin oxide (ITO)-based conductive films have recorded appreciable low resistivity of ~ 10⁻⁴ Ω cm with an

✉ T. M. W. J. Bandara
awijendr@yahoo.com

¹ Department of Physics and Post Graduate Institute of Science, Faculty of Science, University of Peradeniya, Peradeniya, Sri Lanka

² National Institute of Fundamental Studies, Hantana Road, Kandy, Sri Lanka

³ University of West Georgia, Carrollton, USA

⁴ Department of Physics, Georgia State University, Atlanta, USA

optical transmittance of $\sim 80\%$ [9]. However, the preparation of ITOs is relatively costly since indium is an element of shortage [10]. Aluminum-doped zinc oxide (AZO) is a low-cost alternative [11]. Conversely, zinc oxide TCOs prepared by doping cations are not thermally and chemically stable [12]. The electrical conductivity of ITOs becomes low when the temperature is raised above $300\text{ }^{\circ}\text{C}$ at the ambient atmosphere [5, 13].

Fluorine-doped tin oxides (FTOs) are more useful material in optoelectronic devices [14]. FTO films coated on glass substrates give higher electrical conductivity, transparency, and in particular higher temperature tolerance and thus are suitable for a wide range of optoelectronics such as touch screen displays, thin-film photovoltaics, photoelectrochemical solar cells, energy-saving windows, electro-optical and insulating applications [15, 16]. Transparent FTO conducting coatings are very stable under ambient conditions, for instance, they are chemically inert, physically solid and stiff, thermally stable, and more tolerable to physical abrasion [16]. In addition, the production cost of FTO is less than that of indium tin oxide [17]. According to a recent comparative study done by Sarker et al. [12] with FTO, ITO, AZO, and GZO (gallium-doped zinc oxide), FTO emerged as one of most suitable TCOs.

The sheet resistance of FTOs can be improved by increasing the layer thickness but the transparency will be sacrificed. Conversely, when the thickness decreased to improve the transparency, the conductivity suffers, and the situation is tradeoffs. There are some applications where transparency is not very significant; however, the chemical and physical inertness and the conductivity can be critical. For example, metal electrodes cannot be used with corrosive solvents; in such circumstances, FTO is an ideal candidate. Further, most of the supercapacitor electrodes which are prepared on FTO substrates are taking advantage of high conductivity. In solar cell applications, for the preparation of photoelectrodes, both low resistance and high transparency should be considered. For the counter electrode applications of dye-sensitized

solar cells (back contact), the conductivity is more demanding than the transparency. This study aims to introduce a facile and low-cost method to prepare FTO with variable transparency and conductivity suitable for a wide range of applications.

The FTO films were prepared on glass substrates using a simple sequential nebulizer spray pyrolysis method. It allowed the control of layer thickness, thus the sheet resistance and the transmittance based on the number of sequential sprays. In addition to the electrical optical and morphological characterization, prepared FTO films were tested for a quasi-solid-state dye-sensitized solar cell (DSC) by incorporating the FTO films into complete the DSC.

Materials and methods

For the precursor solution preparation, 9.01 g of $\text{SnCl}_2 \cdot 2\text{H}_2\text{O}$ (Sigma-Aldrich, 99%) was added to 400.0 cm^3 (Sigma-Aldrich, 95%) of absolute ethanol, and the mixture was sonicated for 15 min. Then 2.4 g of a saturated aqueous solution of NH_4F (Sigma-Aldrich, 99%) was added to the above solution, and the mixture was sonicated again for about 15 min. Concentrated HCl ($\sim 20.00\text{ cm}^3$) was added to the translucent mixture, making it transparent.

A nebulizer (spray gun) was prepared using two glass droppers, which was used to spray the solution on well-cleaned soda-lime glass plates (microscopic glass slides). An image of the nebulizer spray gun prepared and utilized in this study is shown in Fig. 1a. The spray pyrolysis process is illustrated in Fig. 1b. After preliminary studies, for the deposition of films, the distance between nozzle and substrate was kept fixed at 10 cm .

The precursor solution (40 ml) was sprayed onto a glass substrate ($2.5\text{ cm} \times 2.5\text{ cm}$) towards longitudinal and lateral directions sequentially for 1 min. During the spraying, the temperature of the glass substrate was maintained at $500\text{ }^{\circ}\text{C}$. After spraying, the sample was kept at $\sim 500\text{ }^{\circ}\text{C}$

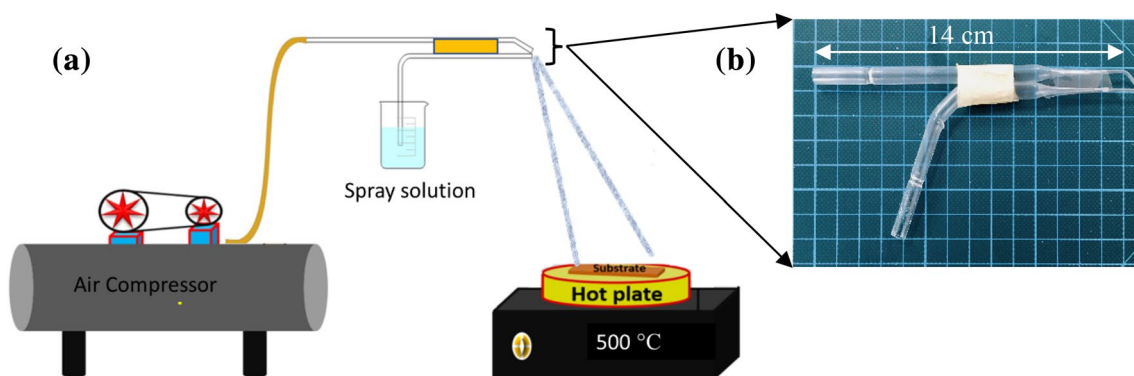


Fig. 1 **a** An illustration of the spraying process (not to a scale) and **b** a photograph of homemade spray gun prepared by two glass droppers

for 1 h. This process, spraying 40 ml of the solution and subsequent heating to 500 °C, is considered one cycle of spray pyrolysis or one-layer preparation. The procedure was repeated several times to get the desired film thickness. For a layer, spray time for each direction (1 min) and the amount sprayed (40 ml) were kept fixed. The number of layers was varied from 1 to 12 in this investigation. Multiple samples were prepared for each composition and the highest conducting sample is selected for further analysis and characterization.

FTOs fabricated in this study were used to prepare quasi-solid-state DSC. The details for the method of preparation of photoelectrode and electrolyte can be found in a published article [18]. The TiO₂ photoelectrode is sensitized with the Ruthenium N719 dye complex. Multilayered (five) photoelectrode is prepared using spin coating on FTO films using TiO₂ P25 nano-powder (particle size 21 nm). The electrolyte is prepared using poly (ethylene oxide) PEO, host polymer, LiI, and tetrahexylammonium iodide binary salts, and the counter electrode is a platinum-coated glass [18].

Table 1 The sheet resistance, resistivity, and conductivity of FTO films prepared by varying the number of sequential deposition cycles

| Number of layers | Sheet resistance ($\Omega \text{ cm}^{-2}$) | Resistivity ($\text{m}\Omega \text{ cm}$) | Conductivity (S cm^{-1}) |
|------------------|---|---|-------------------------------------|
| 1 | 1800.32 | 18.00 | 55.55 |
| 2 | 1400.20 | 28.00 | 35.71 |
| 3 | 969.73 | 29.09 | 34.37 |
| 4 | 729.85 | 29.19 | 34.25 |
| 5 | 573.13 | 28.66 | 34.90 |
| 6 | 365.89 | 21.95 | 45.55 |
| 7 | 188.94 | 13.23 | 75.61 |
| 8 | 75.71 | 6.06 | 165.10 |
| 9 | 52.18 | 4.70 | 212.93 |
| 10 | 25.37 | 2.54 | 394.21 |
| 11 | 15.53 | 1.71 | 585.49 |
| 12 | 9.01 | 1.08 | 924.90 |

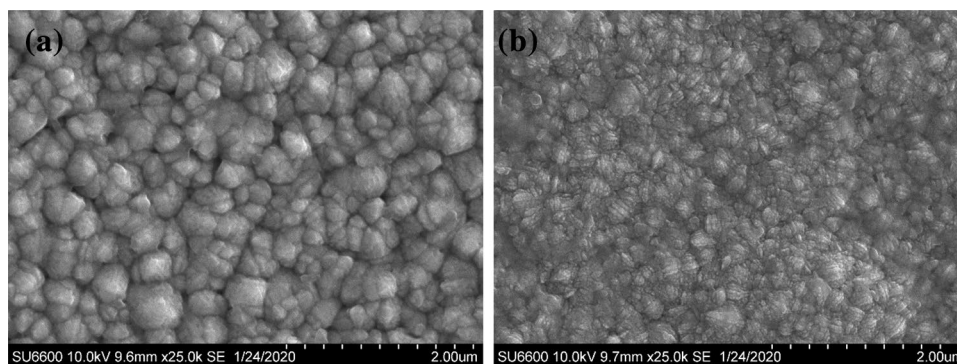
Results and discussion

The sheet resistance, resistivity, and conductivity of the FTO films prepared by varying the number of sequential deposition cycles (or the number of layers) are given in Table 1. The sheet resistance of FTO films increases with the increasing number of spray cycles; this is due to the increasing thickness of the films, which in turn improved the electrical contact between crystallites. The first FTO layer is prepared on a glass substrate is thin but homogeneous compared to other layers of FTO. Therefore, crystallites can more uniformly distribute on the glass substrate and thus resulted in intersections between FTO crystallites which may be responsible for the slightly higher conductivity exhibited by the films with 1 and 2 layers. However, when the number of layers is higher than 5, the conductivity starts to increase. This may be due to improved electrical interconnections between FTO crystallites as a result of pore filling and compact-packing of crystallites.

Further, the conductivity contribution from the outer layers should, in principle, be less than the inner layers due to the rough surface morphology of the outer layers. Therefore, as expected, conductivity increases with increasing numbers of inner layers. The FTOs having more than 10 layers show more or less sheet resistance higher than $25 \Omega \text{ cm}^{-2}$, and thus they are suitable for many applications. The FTO films containing 12 layers showed $9.01 \Omega \text{ cm}^{-2}$, while the FTO film containing 10 layers showed $25.37 \Omega \text{ cm}^{-2}$.

Scanning electron micrographs (SEMs) were investigated to study the morphology of the FTO films fabricated. Figure 2a shows the SEM of the film prepared by 10 sequential spray cycles (10 layers), at the magnification of 25,000. SEMs of the film show compact granular nanostructured FTO crystallites. The films comprised closely packed FTO grains ($\sim 150 \text{ nm}$) as seen in Fig. 2. The larger and compact FTO grains facilitate the charge transfer due to the reduction of crystal boundaries and scattering of carriers. Figure 2b shows an SEM of FTO films prepared by using 12 sequential spray cycles. The FTO crystallites seen in Fig. 2b are

Fig. 2 SEM of the FTO film prepared using **a** 10 number spray cycles and **b** 12 number spray cycles



relatively small and closely packed despite the increased spray coating cycles. This behavior can be due to stockpiling of thickness and constrictions for the grain growth due to the surface roughness of the substrate. The larger FTO grain size can facilitate the charge transfer due to fewer crystal boundaries and reduced carrier transport scattering. Cracks or pinholes are not visible in the films, and thus, such films are suitable for many device applications.

A SEM of the cross section of FTO films prepared using 10 sequential spray pyrolysis cycles is shown in Fig. 3. The average thickness of the FTO films having 10 layers is ~ 964 nm. Therefore, approximately the average thickness of a single layer can be considered as 96.4 nm. The sequential layer deposition method gave reasonable control over layer thickness and sheet resistance. As seen from Fig. 3, the layers coated at different cycles are combined well to form a compact single film of FTO.

The UV–visible transmittance spectrum of the FTO sample (with 10 layers) is shown in Fig. 4. The spectrum indicates that the material has over 65% optical transmittance in the spectral range from 400 to 750 nm, with a maximum of 71% at 660 nm. Bandgap calculation was done using a Tauc plot and the resulted value for an FTO with 10 spray cycles ($25 \Omega \text{ cm}^{-2}$) is 3.7 eV [8].

According to the elemental XRD analysis, the fabricated thin film contains Sn, O, and F. The XRD spectrum of the 10-layer film is illustrated in Fig. 5. Several peaks are visible in the XRD spectrum, which are assigned to SnO_2 crystal planes and corresponding to 2θ values of 26.64° (110), 33.90° (101), 37.95° (200), 51.87° (211), 56.17° (200), 60.05° (310), 61.89° (301).

The current density variation with cell potential is shown in Fig. 6 at three different irradiation times, and the solar cell parameters are listed in Table 2. The efficiency of the solar

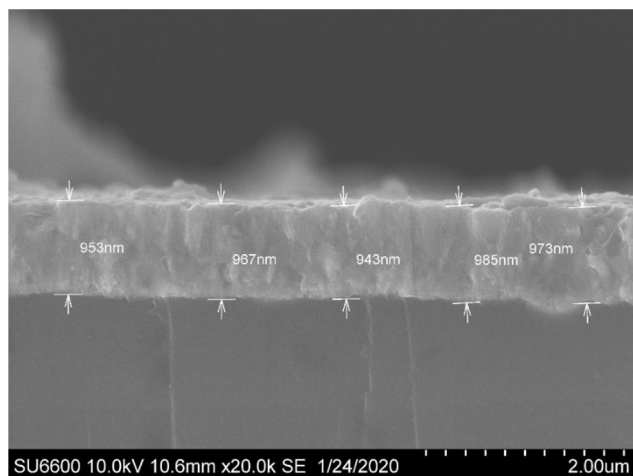


Fig. 3 Cross section of FTO films prepared by nebulizer spray pyrolysis with coating number 10

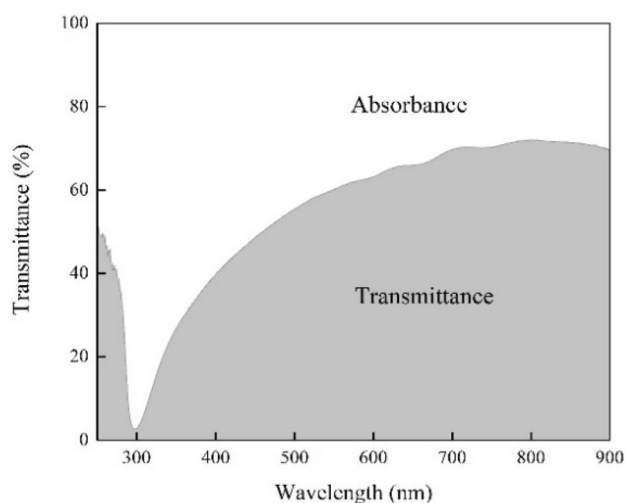


Fig. 4 The transmittance spectroscopy of FTO prepared using 10 spray cycles

cell tested using fabricated FTO was 4.6% and it improves to 4.9% under continued irradiation of about one hour. The DSC shows higher short-term stability within the irradiated time period. The efficiency increase with irradiation time may be resulted from the heating effect. The study exhibits the suitability of the fabricated FTO for DSC application.

Conclusion

The sheet resistance of the FTO films fabricated by sequential nebulizer pyrolysis using a homemade spray gun showed a decrease of sheet resistance and an increase of bulk conductivity with the rise of numbers of cycles. Therefore, the sheet resistance of an FTO can be tuned by varying the

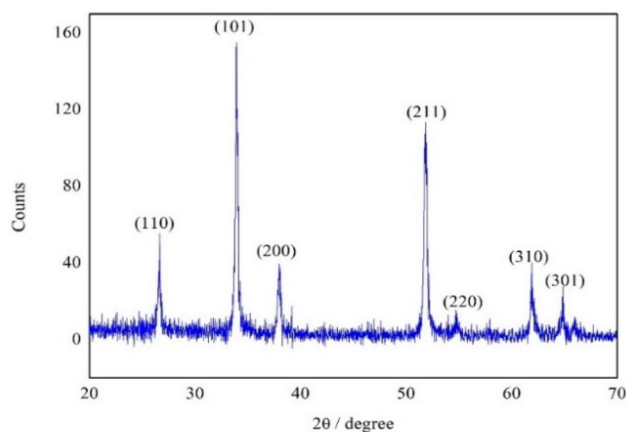


Fig. 5 X-ray diffraction pattern for the FTO glass with 10 spray cycles

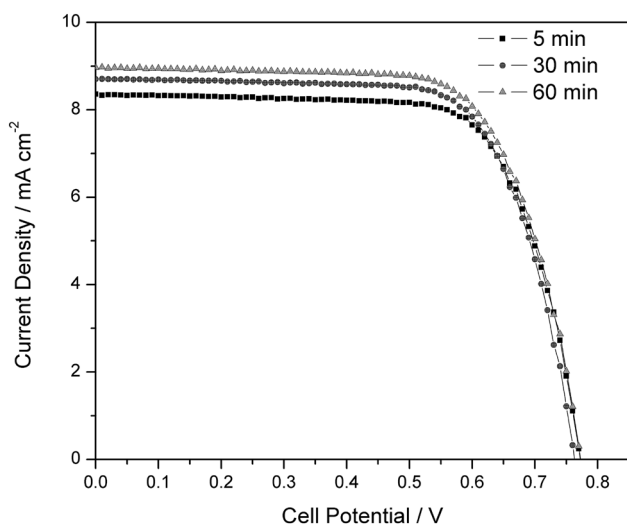


Fig. 6 Current density variation as a function of cell potential for three different illumination times for the DSC

Table 2 Solar cell performance parameters

| Time (min) | J_{sc} (mA cm ⁻²) | V_{oc} (V) | Efficiency (%) |
|------------|---------------------------------|--------------|----------------|
| 05 | 8.36 | 0.78 | 4.6 |
| 30 | 8.70 | 0.77 | 4.8 |
| 60 | 8.97 | 0.78 | 4.9 |

number of spray cycles. Films prepared by 10 spray cycles showed sheet resistance of $\sim 25 \Omega \text{ cm}^{-2}$ and optical bandgap of $\sim 3.7 \text{ eV}$. For the visible region, the average transmittance of the film is 70%. Samples showed crack and pinhole free surface morphology. The maximum efficiency of quasi-solid-state DSC fabricated is $\sim 4.9\%$. The fabricated FTO is suitable to prepare photoelectrodes for DSC application.

Data availability Data will be made available upon reasonable request.

Compliance with ethical standards

Conflict of interest The authors declare that they have no known competing financial interests or no conflicts of interest in this paper.

References

1. D. Solís-Cortés, R. Schrebler, E. Navarrete-Astorga, M. López-Escalante, F. Martín, J.R. Ramos-Barrado, E.A. Dalchiele, J. Alloys Compd. **808**, 151776 (2019). <https://doi.org/10.1016/j.jallcom.2019.151776>
2. T. Minami, MRS Bull. **25**, 38–44 (2000)
3. B. Han et al., Adv. Mater. **26**(6), 873–877 (2014). <https://doi.org/10.1002/adma.201302950>
4. A.C. Zhou, ACS Nano **4**(1), 11–14 (2010). <https://doi.org/10.1021/nn901903b>
5. S. Abdullahi, A.U. Moreh, B. Hamza, U. Sadiya, Z. Abdullahi, M.A. Wara, H. Kamaluddeen, M.A. Kebbe, U.F. Monsurat, IJIAS. **9**, 947–955 (2014)
6. L. Dominici, F. Michelotti, T.M. Brown et al., Opt. Express **17**(12), 10155–10167 (2009). <https://doi.org/10.1364/OE.17.010155>
7. S.-W. Feng, Y.-H. Wang, C.-Y. Tsai, T.-H. Cheng, H.-C. Wang, Sci. Rep. **10**(1), 1–8 (2020). <https://doi.org/10.1038/s41598-020-67274-1>
8. T. Minami, Semicond. Sci. Technol. **20**(4), S35 (2005). <https://doi.org/10.1088/0268-1242/20/4/004>
9. Z. Chen, W. Li, R. Li, Y. Zhang, G. Xu, H. Cheng, Langmuir **29**(45), 13836–13842 (2013). <https://doi.org/10.1021/la4033282>
10. L.H. Lalasari, T. Arini, L. Andriyah, F. Firdiyono, A.H. Yuwono, AIP Conf. Proc. **1964**(1), 020001 (2018). <https://doi.org/10.1063/1.5038283>
11. T. Dhakal et al., Sol. Energy **86**(5), 1306–1312 (2012). <https://doi.org/10.1016/j.solener.2012.01.022>
12. S. Sarker, H.W. Seo, Y.K. Jin, M.A. Aziz, D.M. Kim, Mater. Sci. Semicond. Process. **93**, 28–35 (2019). <https://doi.org/10.1016/j.mssp.2018.12.023>
13. B. Russo, G.Z. Cao, Appl. Phys. A. **90**(2), 311–315 (2008). <https://doi.org/10.1007/s00339-007-4274-4>
14. D. Keller, H. Barad, E. Rosh-Hodesh, A. Zaban, D. Cahen, MRS Commun. **8**(3), 1358–1362 (2018). <https://doi.org/10.1557/mrc.2018.179>
15. A. Purwanto, H. Widiyandari, A. Jumari, Thin Solid Films **520**(6), 2092–2095 (2012). <https://doi.org/10.1016/j.tsf.2011.08.041>
16. N.S. Khalid, W. Zaki, W. Suhaimizan, M.K. Bin Ahmad, Adv. Mater. Res. **1109**, 11–14 (2015). <https://doi.org/10.4028/www.scientific.net/AMR.1109.11>
17. S. Saehana, Z. Arifin, Nasar, IOP Conf. Ser. Mater. Sci. Eng. **622**(1), 012032 (2019). <https://doi.org/10.1088/1757-899X/622/1/012032>
18. T.M.W.J. Bandara, L. DeSilva, J. Ratnasekera, K. Hettiarachchi, A. Wijerathna, M. Thakurdesai, J. Preston, I. Albinsson, B. Melander, Renew. Sust. Energ. Rev. **103**, 282–290 (2019). <https://doi.org/10.1016/j.rser.2018.12.052>